Reduction in Near-Surface Wind Speeds With Increasing CO$_2$ May Worsen Winter Air Quality in the Indo-Gangetic Plain

Fabien Paulot[1] ORCID**, Vaishali Naik[1]** ORCID**, and Larry W. Horowitz[1]** ORCID

[1]Geophysical Fluid Dynamics Laboratory, National Oceanic and Atmospheric Administration, Princeton, NJ, USA

Abstract We analyze the relationship between fine particulate matter ($PM_{2.5}$) and meteorology in winter in the Indo-Gangetic Plain (IGP). We find that the concentration of $PM_{2.5}$ exhibits similar increase with decreasing surface wind speed in 15 out of 18 cities considered. Using this observed relationship, we estimate that the reduction of surface wind speed with increasing CO_2 simulated by models participating in the Coupled Model Intercomparison Project Phase 6 will result in higher average wintertime $PM_{2.5}$ concentrations (1% per degree K of global warming) and more frequent high-pollution events. This observation-based estimate is qualitatively consistent with the simulated response of black carbon to global warming inferred from the AerChemMIP ssp370SST and ssp370pdSST experiments. We hypothesize that a reduction in the frequency and intensity of western disturbances with increasing CO_2 may contribute to the reduction in the surface wind in the IGP.

Plain Language Summary The Indo-Gangetic Plain, home to over 800 million people, experiences among the most elevated concentrations of fine particulate matter in the world. Such high levels of air pollution are estimated to reduce average life expectancy by several years. Air quality is especially poor in wintertime, in part due to meteorological conditions such as slow wind speeds that favor the accumulation of air pollutants near the surface. CMIP6 models project that increasing CO_2 will cause a reduction in surface wind speed in the Indo-Gangetic Plain. We show that this reduction in wind speed will result in higher wintertime $PM_{2.5}$ concentration (1%/K) and more frequent high-$PM_{2.5}$ days. This CO_2 penalty highlights the need for stringent air pollution controls in this region.

1. Introduction

The Indo-Gangetic Plain (IGP) stretches from Pakistan to Bangladesh across Northern India. A major center for wheat and rice production, it is home to over 800 million people (Chauhan et al., 2012). The IGP experiences some of the highest concentrations of airborne fine particulate matter ($PM_{2.5}$) in the world (Gargava & Rajagopalan, 2015a; Gargava & Rajagopalan, 2015b; Guttikunda et al., 2014; Jethva et al., 2019; Srinivas Bikkina and August Andersson and Elena N. Kirillova and Henry Holmstrand and Suresh Tiwari and A. K. Srivastava and D. S. Bisht and Örjan Gustafsson, 2019; Singh et al., 2017; K. K. Lee & Greenstone, 2021b). High local anthropogenic emissions associated with waste and crop residue burning, transportation, industry, and power generation are the primary cause for the poor air quality in the region (Singh et al., 2021). The topography of the IGP region, bordered to the North by the Himalayan mountain range and to the South by the Chota Nagpur and Deccan plateaux, encourages air stagnation, which further exacerbates air pollution (Jethva et al., 2005; Mhawish et al., 2020; Ojha et al., 2020; V. S. V. S. Nair et al., 2007; M. M. Kumar et al., 2015; Yadav et al., 2015).

Exposure to $PM_{2.5}$ is associated with increased risk of cardiovascular and respiratory diseases (Roth et al., 2018). In the states of Delhi and Uttar Pradesh, home to over 245 million people (S. S. Kumar et al., 2019), the annual $PM_{2.5}$ concentration exceeds the recommendations (5 µg m^{-3}) by the World Health Organization (2021) by more than 20-fold and is estimated to cause a loss of life expectancy of ≃10 years (K. Lee & Greenstone, 2021a). Unlike other major population centers in Europe, the United States, and China, air pollution has been worsening in the IGP over the last two decades (M. Kumar et al., 2018; M. Nair et al., 2022; Vohra et al., 2021). Turnock et al. (2020) recently showed that $PM_{2.5}$ concentrations are projected to keep increasing by 10%–40% in South Asia over the next decades based on simulations in support of the Coupled Model Intercomparison Project 6 (CMIP6, Eyring et al. (2016)) using different Shared socio-economic pathways (SSPs). The simulated changes in $PM_{2.5}$ exhibit high correlations with precursor emissions, which highlights the importance of emission controls to curb air pollution. Such controls have recently been proposed by the Indian Government under the National

Clean Air Program (NCAP) with the aim to reduce air pollution by 20%–30% by 2024 relative to 2017 levels (Ganguly et al., 2020).

Air pollution in IGP is especially elevated in winter (DJF) (Gani et al., 2019; Haque & Singh, 2017; Murari et al., 2017; Schnell et al., 2018) when low wind speeds, shallow boundary layer heights and strong temperature inversions have been shown to favor stagnant conditions that promote the accumulation of $PM_{2.5}$ near the surface (M. Kumar et al., 2015; V. S. Nair et al., 2007; Ojha et al., 2020; Schnell et al., 2018; Singh et al., 2021).

The impact of climate change on the meteorological conditions in the IGP and the implications for air quality remain uncertain. Horton et al. (2014) found that climate change would increase the air stagnation index (ASI), a metric that exhibits a positive correlation with $PM_{2.5}$ in the United States. In contrast, Wu et al. (2019) and Li et al. (2021) found that synoptic conditions (e.g., location of the subtropical jet) correlated with elevated $PM_{2.5}$ become less frequent with global warming. The lack of consensus regarding the relationship between meteorology and $PM_{2.5}$ can be partly attributed to the lack of long-term $PM_{2.5}$ observations and the sparseness of $PM_{2.5}$ monitoring stations in the IGP, the majority of which are located in the Delhi region. In addition, the coupling between meteorological conditions at the surface and in the upper atmosphere is weak in the winter over the IGP, which reduces the predictive power of synoptic meteorology-based indicators such as the ASI for high-pollution episodes in this region (Schnell et al., 2018).

Here we analyze daily wintertime (DJF) observations collected in the Indian portion of the IGP from December 2014 to February 2020 to characterize the relationship between surface meteorological conditions and $PM_{2.5}$. We then use these observation-based relationships to quantify how changes in meteorology associated with climate change will impact winter $PM_{2.5}$ concentrations in the IGP. Finally we show that this meteorological response is qualitatively captured by CMIP6 models.

2. Observed Relationship Between Meteorology and $PM_{2.5}$

Hourly $PM_{2.5}$ concentrations are obtained from India's Central Pollution Control Board (Government of India, 2021) and from the U.S. Embassy and Consulates' air quality monitors (U.S. Department of State, 2021) from December 2014 to February 2020. Note that very few $PM_{2.5}$ observations are available in the IGP prior to this period. We average the hourly data to construct daily timeseries, filtering the data as follows: (a) exclude periods when more than 12 consecutive observations are identical; (b) exclude hourly data that deviate from the daily mean by more than 3 standard deviation (zscore ≥ 3, Mogno et al. (2021)); (c) exclude days with fewer than 12 measurements (Mogno et al., 2021); (d) exclude daily data which differ from the annual mean by more than 5 standard deviations (zscore ≥ 5).

We focus our analysis on daily $PM_{2.5}$ timeseries at stations with at least three valid winter seasons, where a valid winter season is defined as having valid $PM_{2.5}$ observations for more than 45 days. In the Indian portion of the IGP, which comprises the states of Punjab, Haryana, National Capital Territory of Delhi, Uttar Pradesh, Bihar, Jharkhand, and West Bengal, 18 cities have one or more stations that meet the aforementioned criteria (Figure 1, Table S1 in Supporting Information S1). Four of these cities are located in the near vicinity of New Delhi, while no city meets the criteria in the state of Jharkhand. We perform the analysis on daily anomalies relative to the winter mean to reduce the impact of interannual variability and trends associated with emission changes.

Figure 2 summarizes the correlation between $PM_{2.5}$ and meteorological variables on a daily timescale (Table S2 in Supporting Information S1). Following previous studies (Li et al., 2021; Schnell et al., 2018; Wu et al., 2019), we consider collocated boundary layer height, near-surface wind speed (sfcWind) and temperature (t2m), surface pressure, precipitation, sea level pressure, relative humidity, and temperature inversion (INV, the difference between the 850 mb and surface (2m) temperature) – a proxy for the lower atmospheric stability (Ramanathan et al., 2005). Because meteorological observations are not available at all stations, all meteorological data are obtained from ECMWF Reanalysis fifth Generation (ERA5, 0.25° resolution, Hersbach et al. (2020)). Figure 2 shows that boundary layer height and INV are significantly correlated ($p < 0.01$) with $PM_{2.5}$ in all cities, with average correlations of −0.46, 0.37, respectively. sfcWind exhibits significant correlation with $PM_{2.5}$ in 17 out of 18 cities, with an average correlation of −0.43. The correlation of $PM_{2.5}$ with boundary layer height, INV, and sfcWind are consistent with the enhancement of $PM_{2.5}$ under stagnant conditions. Other collocated meteorological variables, that is, surface pressure, sea level pressure, relative humidity, and precipitation exhibit much weaker correlation with $PM_{2.5}$. We also find significant correlation between $PM_{2.5}$ and daily t2m in 15 out of 18 cities. However, this relationship is likely to be partly driven by changes in residential emissions, the largest contributor
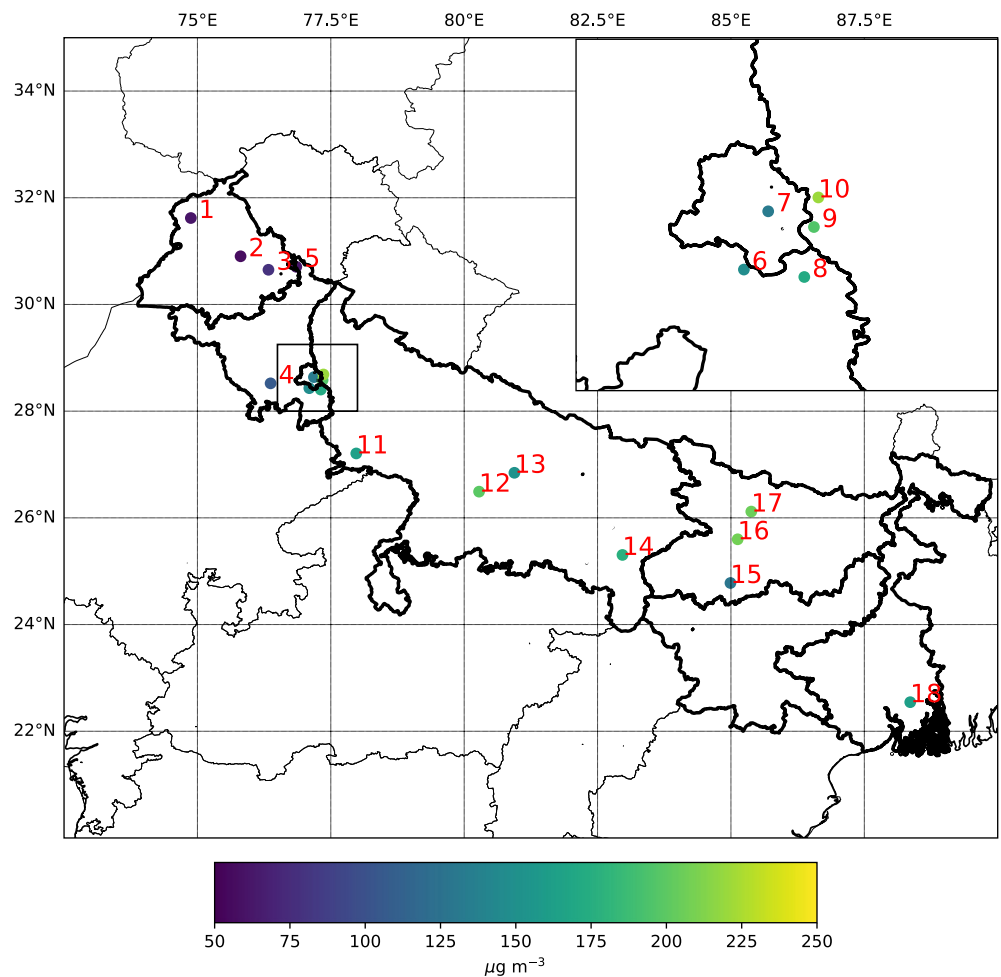
Figure 1. Location of the cities used in this study 1. Amritsar [Punjab]; 2. Ludhiana [Punjab]; 3. Mandi Gobindgarh [Punjab]; 4. Rohtak [Haryana]; 5. Panchkula [Haryana]; 6. Gurugram [Haryana]; 7. Delhi [NCT of Delhi]; 8. Faridabad [Haryana]; 9. Noida [Uttar Pradesh]; 10. Ghaziabad [Uttar Pradesh]; 11. Agra [Uttar Pradesh]; 12. Kanpur [Uttar Pradesh]; 13. Lucknow [Uttar Pradesh]; 14. Varanasi [Uttar Pradesh]; 15. Gaya [Bihar]; 16. Patna [Bihar]; 17. Muzaffarpur [Bihar]; 18. Kolkata [West Bengal]. Locations are color coded by the average DJF $PM_{2.5}$ concentration in the associated city in $\mu g\ m^{-3}$ over the 2015–2020 period. The states that comprise the IGP are highlighted in bold.

to $PM_{2.5}$ in wintertime (Singh et al., 2021), rather than a purely meteorological effect. In the following, we focus on the relationship of $PM_{2.5}$ with daily sfcWind and INV, which exhibit highest correlation with $PM_{2.5}$ and are available from many models which contributed to CMIP6. This daily variations of INV, sfcWind and $PM_{2.5}$ are illustrated in Figure S1 of Supporting Information S1. We do not consider boundary layer height because it is available from fewer CMIP6 models than sfcWind, with which it exhibits high correlation (>0.5) in 16 out of 18 cities. In contrast, the correlation between sfcWind and INV is not significant at the 0.01 level in 14 out of 18 cities. The average sfcWind and INV over the 2010–2018 period are shown in Figures S2 and S3 of Supporting Information S1.

To explore the relationships of $PM_{2.5}$ with sfcWind and INV, we bin observations by deciles of the sfcWind and INV distributions (independently, see Tables S3 and S4 in Supporting Information S1). Figures 3a and 3b show the anomaly in DJF $PM_{2.5}$ for each sfcWind and INV decile relative to the DJF average for each IGP city. We find significant negative and positive associations ($p < 0.01$) between $PM_{2.5}$ and sfcWind and INV deciles, respectively in all cities except Kolkata, Rohtak, and Mandi Gobindgarh for sfcWind deciles. On average, the concentration of $PM_{2.5}$ differs by close to a factor of two between the lower and upper sfcWind and INV deciles.

Figures 3c and 3d show the conditional cumulative probability of high-$PM_{2.5}$ days (upper quartile) given sfcWind and INV deciles, respectively. On average, 50% and 75% of the worst air quality days occur for sfcWind in the
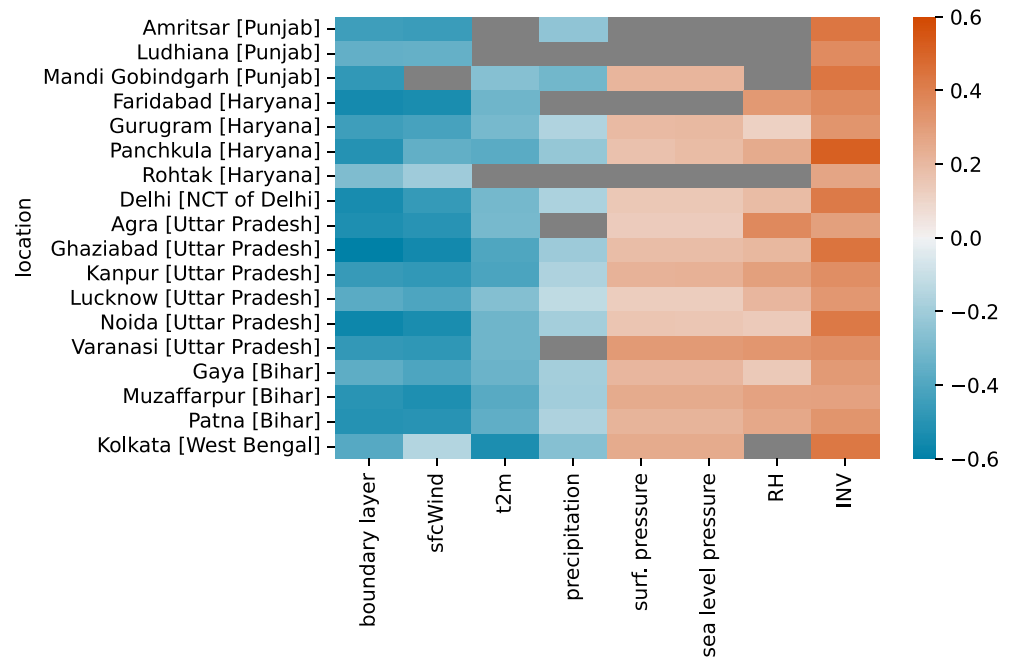
Figure 2. Correlation between meteorological variables and $PM_{2.5}$ for cities in the Indo-Gangetic Plain. Only significant correlations ($p < 0.01$) are shown.

lowest three and five deciles, respectively. In particular, the probability of a high-$PM_{2.5}$ day is increased two-fold at the slowest wind speed deciles. No significant relationship between wind speed decile and the probability of a high-$PM_{2.5}$ day is found at Kolkata, Rohtak, and Mandi Gobindgarh. The probability of a poor air quality day is less sensitive to INV than to sfcWind, as indicated by the smaller departure from the 1:1 line (Figure 3d).

In winter, the IGP circulation is dominated by nortwesterly winds (Figure S2 in Supporting Information S1). This stable circulation pattern tends to reduce the sensitivity of $PM_{2.5}$ to regional sources (Singh et al., 2021) and results in a West-East increase in $PM_{2.5}$ (Figure 1 and Mogno et al. (2021)). This circulation pattern may also contribute to the similarity in the relationship of $PM_{2.5}$ to surface meteorological conditions across cities. Mandi Gobindgarh (northeast of IGP) and Kolkata (southwest of IGP) are located on the edge of the IGP, which may increase their sensitivity to the variability of local sources. In addition, Kolkata is located ≃200 km from the sea and air quality in the city is modulated by sea/land breeze activity (Verma et al., 2016), which we do not account for in our analysis. More information would be required to further explore the lack of significant relationship between sfcWind decile and $PM_{2.5}$ at Rohtak in spite of its proximity to Delhi (Figure 1). We note that Rohtak has the fewest number of observations across all the cities analyzed here (Table S1 in Supporting Information S1), which may contribute to the less robust relationship between sfcWind and $PM_{2.5}$ at this site.

The observed relationship between $PM_{2.5}$ and INV/sfcWind may also help diagnose model biases. For instance, Figure S4 in Supporting Information S1 shows the simulated relationship between INV/sfcWind and $PM_{2.5}$ in the GFDL ESM4.1 model (Dunne et al., 2020; Horowitz et al., 2020). The model captures well the relationship between sfcWind and $PM_{2.5}$ in the interior of the IGP but overestimates the impact of sfcWind at Kolkata. The model also generally underestimates the impact of INV on $PM_{2.5}$, which may indicate an underestimate of the impact of aerosols on the lower tropospheric stability.

3. Change in Local Meteorology With Climate Change and Implication for $PM_{2.5}$

We use simulations performed for CMIP6 to estimate the impact of global warming on sfcWind and INV in the IGP. We first analyze changes in daily sfcWind and INV in the 1pctCO2 experiment (1% per year increase of the atmospheric concentration of CO_2) relative to preindustrial conditions (piControl). This allows to isolate the impact of CO_2-induced global warming from other factors that can impact local meteorology, such as changes in land-use (e.g., urbanization (Civerolo et al., 2007; Huszar et al., 2020; Tao et al., 2015) or non–CO_2 climate
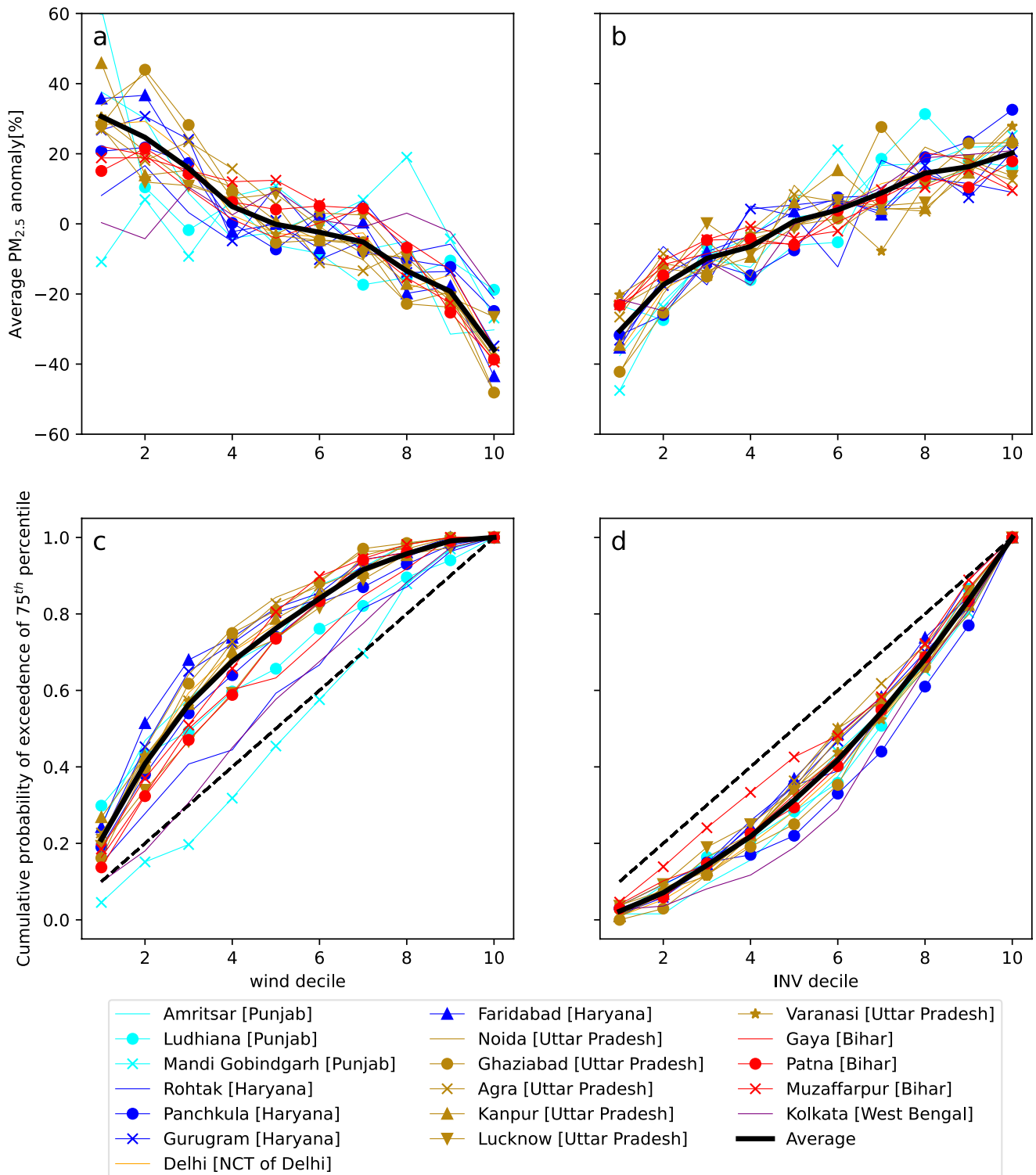
Figure 3. Average relationship of $PM_{2.5}$ with surface wind speed and temperature inversion (INV) deciles in DJF for cities in the Indo-Gangetic Plain. Panels a and b show the average anomaly in $PM_{2.5}$ concentration relative to the seasonal mean for each sfcWind (panel a) and INV decile (panel b). Panels c and d show the conditional cumulative probability of exceeding $PM_{2.5}$ 75th percentile given sfcWind and INV decile. Cities are ordered from West to East and color coded by state. The solid black line shows the average response across all cities. We exclude Rohtak, Mandi Gobindgarh, and Kolkata for wind speed, as no significant relationship with $PM_{2.5}$ is observed for these cities. The dashed black line (panels c and d) shows the expected distribution of $PM_{2.5}$ if it were independent of sfcWind and INV (i.e., uniform distribution).

forcers (Fosu et al., 2017)). Details about the 26 models used for sfcWind and 11 models for INV can be found in Table S5 of Supporting Information S1.

For each model, we first calculate the sfcWind and INV deciles under preindustrial conditions in each grid cell using at least 150 years of the piControl experiment. We then regress the frequency of each decile in the 1pctCO2 experiment (150 years) against the global mean temperature change using ordinary least squares. To reduce the impact of natural variability, we apply a 20-year running mean prior to calculating the regression coefficients. To facilitate comparison across models, model outputs are regridded to a common $1° \times 1°$ grid using the Earth System Modeling Framework conservative algorithm.

Figure S5 in Supporting Information S1 shows that most CMIP6 models project that CO_2-induced global warming tends to shift the distribution of sfcWind toward slower wind speeds. The response is consistent in sign over much of the IGP, except in Punjab, where no significant change is found. The largest increase in slow wind speed days is found in Uttar-Pradesh. Figure S6 in Supporting Information S1 illustrates this change in the sfcWind distribution in the GFDL ESM4.1 model in the different cities shown in Figure 1. In contrast, changes in the distribution of daily INV are more geographically heterogeneous and less robust (Figure S7 in Supporting Information S1). Robust changes are only identified in the Northwest and Southeast portions of the IGP where the frequency of low and high INV days is found to increase and decrease, respectively.

The weather in Northern India in winter is modulated by the passage of western disturbances (WD). These cyclonic storms (10–26/year in DJF (Midhuna et al., 2020)) originate over the Mediterranean, Caspian and Black Seas and move eastwards across Northwestern India following the westerlies (Dimri et al., 2015). Some WDs bring precipitation and rapid surface wind-speed in the IGP thus modulating air quality (Pawar et al., 2015). For instance, low WD activity in December 2015 likely contributed to extremely high air pollution in New Delhi (Basu et al., 2017). Following Midhuna et al. (2020) we diagnose the change in WD activity using the Western disturbance index (WDI), the difference in geopotential heights between 850 and 200 hPa over the region 25–40°N 60–80°E. Figure S8 in Supporting Information S1 shows that the WDI is decreasing with global warming. This decrease is also supported by the simulated reduction in wintertime precipitation over the IGP (Figure S9 in Supporting Information S1), most of which is contributed by winter disturbances (Hunt et al., 2018). It is also consistent with the detailed analysis of Hunt et al. (2019), who showed that CMIP5 models projected a decrease in both the frequency and intensity of WDs with radiative forcing. This suggests that more research is needed to characterize how changes in WD activity may contribute to the projected increase in the prevalence of calm conditions.

Our analysis only addresses the impact of increasing CO_2 on INV and sfcWind. To assess how changes in non-CO_2 forcing agents including anthropogenic aerosols may alter meteorological conditions, we analyze simulated changes in sfcWind and INV over the historical period and under the future ssp370 scenario. The ssp370 scenario follows the RCP7.0 global forcing pathway with SSP3 socioeconomic conditions (O'Neill et al., 2013; van Vuuren et al., 2013) and corresponds to weak climate change and air quality mitigation. Under the ssp370 scenario, surface $PM_{2.5}$ concentrations in South Asia are projected to increase by 40% relative to 2005–2014 conditions by 2060 and then decrease for the remainder of the 21st century with 2100 concentrations exceeding present-day concentrations by $\simeq 20\%$ (Turnock et al., 2020). We find that the relationship between changes in the sfcWind distribution and global temperature is similar to that derived from the idealized 1pctCO2 simulation (Figures S5 and S10 in Supporting Information S1). In contrast, we find that the response of INV is much stronger (Figures S7 and S11 in Supporting Information S1), consistent with previous studies (Gao et al., 2022; Hingmire et al., 2021; Ramanathan et al., 2005; Yang et al., 2016), which have demonstrated that higher anthropogenic aerosols tend to increase atmospheric stability.

To estimate the impact of the reduction in wind speed on $PM_{2.5}$ concentrations associated with increasing CO_2, we multiply the change in the frequency of each sfcWind decile per degree global warming (Figure S5 in Supporting Information S1) by the observed anomaly in $PM_{2.5}$ in this sfcWind decile (Figure 3a, black line). Figure 4a shows that the change in sfcWind is projected to result in an increase in $PM_{2.5}$ of $\simeq 1\%/K$ over much of the IGP. Similarly, we estimate that the change in the sfcWind distribution will increase the frequency of conditions conducive to high-$PM_{2.5}$ episodes (75th percentile) by $\simeq 4\%/K$ (Figure 4b) or sfc$\simeq 1$ day per season per K.

Another estimate of the impact of changes in meteorological conditions with global warming on $PM_{2.5}$ may be derived independently by comparing the concentration of black carbon simulated by CMIP6 models in the
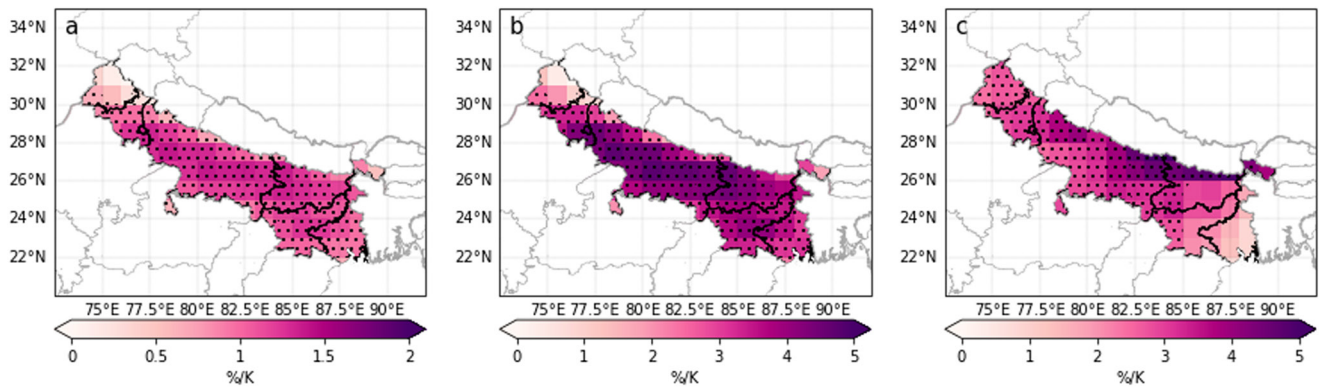
Figure 4. Change in surface $PM_{2.5}$ (a) and probability of exceeding the present-day 75th percentile in $PM_{2.5}$ (b) estimated from the changes in surface wind speed in the 1pctCO2 experiment. The change in BC in the ssp370SST relative to ssp370pdSST experiment is shown in panel (c). All changes are normalized by the global surface temperature change. Stippling indicates regions where changes are statistically significant ($p < 0.01$) and agree on the sign for at least 70% of the models.

ssp370SST and ssp370pdSST experiments, conducted as part of the Aerosol Chemistry Model Intercomparison Project (Collins et al., 2017). The ssp370SST experiment follows the ssp370 scenario with sea surface temperature (SST) and sea ice concentrations (SIC) prescribed from coupled-model ssp370 simulations. The ssp370pdSST experiment follows the same set up except that SST and SIC are taken from the simulated 2005–2014 mean from the associated coupled model simulation. The difference between ssp370SST and ssp370pdSST reflects the impact of increasing sea surface temperature under the ssp370 scenario. We focus on black carbon rather than $PM_{2.5}$ as the sole sources of black carbon are prescribed emissions and thus identical between the two experiments. As a result, differences in surface black carbon between the two runs are expected to be primarily associated with differences in meteorology between the two scenarios. The six models used for this analysis are listed in Table S6 of Supporting Information S1.

Figure 4c shows the average change in surface black carbon simulated in the ssp370SST relative to its concentration in ssp370pdSST regressed against the global change in surface temperature. Similar to our analysis of sfcWind and INV quantiles, model outputs are regridded to a common $1° × 1°$ grid using the Earth System Modeling Framework conservative algorithm and we apply a 20-year running mean to BC concentrations prior to calculating the regression coefficients. The estimated response ranges from 1 to over 5%/K, which is qualitatively consistent with the response of $PM_{2.5}$ inferred from wind speed changes (Figure 4a). However, the sensitivity of surface black carbon to meteorological changes is generally 1.5 to 2× stronger. This stronger response may be partly explained by differences in the response of sfcWind and INV in the ssp370 scenario relative to the 1pctCO2 run.

Both estimates suggest that global warming tends to favor meteorological conditions that are conducive to higher wintertime $PM_{2.5}$ in the IGP. In contrast, Li et al. (2021) recently showed that changes in synoptic conditions diagnosed from the zonal wind speed at 250 hPa associated with climate change will decrease the likelihood of poor winter air quality events in Delhi. This discrepancy may stem in part from the complex coupling between upper atmospheric conditions and surface meteorology in the IGP in winter (Schnell et al., 2018). More $PM_{2.5}$ observations (e.g., outside of urban centers) are needed to better characterize the interactions between meteorology and $PM_{2.5}$ and thus improve future $PM_{2.5}$ projections.

4. Conclusion

The Indo-Gangetic Plain is one of the most polluted regions in the world. The concentration of $PM_{2.5}$ is especially high in winter, frequently exceeding Word Health Organization recommendations by more than an order of magnitude. Such high levels of $PM_{2.5}$ are primarily driven by local and regional precursor emissions and modulated by meteorology. We focus here on the observed relationship of surface wind speed and temperature inversion with $PM_{2.5}$. We show that the frequency of low-wind episodes in the IGP is projected to increase with increasing CO_2, resulting in an increase in both the average wintertime $PM_{2.5}$ (1% per K of global warming) and the likelihood of high $PM_{2.5}$ episodes. In contrast, changes in temperature inversion associated with CO_2-induced

global warming are small. We show that such increase in PM$_{2.5}$ in response to future wind speed changes is qualitatively consistent with, although generally weaker than, the model-simulated sensitivity of black carbon to meteorological changes simulated under the ssp370 scenario. In the near-term, the reduction in sfcWind associated with global warming is expected to have a small impact on PM$_{2.5}$ relative to that of projected emission changes (−20 to +40% change in PM$_{2.5}$ over the next 20 years in South Asia depending on the forcing socioeconomic pathway (Turnock et al., 2020)). By the end of the century, global mean surface temperature are projected to rise by as much as 5°C (for a very high greenhouse gas emission but strong pollution control scenario, ssp585 (Tebaldi et al., 2021),). Our work suggests that under such a scenario, the reduction in sfcWind would significantly worsen air quality in the IGP (+5% in DJF PM$_{2.5}$ and 20% increase in the frequency of meteorological conditions conducive to high pollution episodes). This suggests that meteorological changes associated with global warming may require stronger reductions in anthropogenic emissions than expected to achieve lasting improvements in air quality in the IGP. We further show that such emission reductions would also benefit air quality by reducing the lower atmospheric stability.

More research is needed to understand the mechanism that results in the projected increase in the prevalence of calm conditions in the IGP in winter. Here, we hypothesize that reduction in the frequency and/or intensity of western disturbances may contribute to this change. Besides air quality, western disturbances have many well-known impact for agriculture and hydrology in the IGP (Dimri et al., 2015). Their influence on air quality further highlights the need for additional research to characterize the response of western disturbances to climate change (Hunt et al., 2019).

Data Availability Statement

Open Research Observations can be downloaded from https://app.cpcbccr.com/ccr/%23/caaqm%2Ddashboard/caaqm%2Dlanding/data and from https://www.airnow.gov/international/us-embassies-and-consulates/ (New Delhi, Chennai, Kolkata, Mumbai). ERA5 reanalysis can be obtained at https://doi.org/10.24381/cds.adbb2d47. CMIP6 model output can be obtained at https://esgf-node.llnl.gov/search/cmip6/. Models used in this study are listed in Tables S5 and S6 of Supporting Information S1. We acknowledge the use of the following open source software: Python 3.8, xarray (Hoyer & Hamman, 2017), pandas (Reback et al., 2021), cartopy (Elson et al., 2020), matplotlib (Caswell et al., 2021), and xesmf (Zhuang et al., 2021).

References

Basu, S., Bieniek, P. A., & Deoras, A. (2017). An investigation of reduced Western disturbance activity over northwest India in November - December 2015 compared to 2014 - A case study. *Asia-Pacific Journal of Atmospheric Sciences*, *53*(1), 75–83. https://doi.org/10.1007/s13143-017-0006-7

Caswell, T. A., Droettboom, M., Lee, A., De Andrade, E. S., Hunter, J., & Hoffmann, T. P. (2021). matplotlib/matplotlib: Rel: V3.4.2. Zenodo.

Chauhan, B. S., Mahajan, G., Sardana, V., Timsina, J., & Jat, M. L. (2012). Productivity and sustainability of the rice–wheat cropping system in the indo-gangetic plains of the indian subcontinent. In *Advances in agronomy* (pp. 315–369). Elsevier. https://doi.org/10.1016/b978-0-12-394278-4.00006-4

Civerolo, K., Hogrefe, C., Lynn, B., Rosenthal, J., Ku, J.-Y., Solecki, W., et al. (2007). Estimating the effects of increased urbanization on surface meteorology and ozone concentrations in the New York city metropolitan region. *Atmospheric Environment*, *41*(9), 1803–1818. https://doi.org/10.1016/j.atmosenv.2006.10.076

Collins, W. J., Lamarque, J.-F., Schulz, M., Boucher, O., Eyring, V., Hegglin, M. I., et al. (2017). AerChemMIP: Quantifying the effects of chemistry and aerosols in CMIP6. *Geoscientific Model Development*, *10*(2), 585–607. https://doi.org/10.5194/gmd-10-585-2017

Dimri, A. P., Niyogi, D., Barros, A. P., Ridley, J., Mohanty, U. C., Yasunari, T., & Sikka, D. R. (2015). Western disturbances: A review. *Reviews of Geophysics*, *53*(2), 225–246. https://doi.org/10.1002/2014rg000460

Dunne, J. P., Horowitz, L. W., Adcroft, A. J., Ginoux, P., Held, I. M., John, J. G., et al. (2020). The GFDL Earth system model version 4.1 (GFDL-ESM 4.1): Overall coupled model description and simulation characteristics. *Journal of Advances in Modeling Earth Systems*. https://doi.org/10.1029/2019ms002015

Elson, P., Andrade, E. S. D., Hattersley, R., Campbell, E., May, R., Dawson, A., et al. (2020). Scitools/cartopy: Cartopy 0.18.0. Zenodo. https://doi.org/10.5281/ZENODO.3783894

Eyring, V., Bony, S., Meehl, G. A., Senior, C. A., Stevens, B., Stouffer, R. J., & Taylor, K. E. (2016). Overview of the coupled model intercomparison project phase 6 (CMIP6) experimental design and organization. *Geoscientific Model Development*, *9*(5), 1937–1958. https://doi.org/10.5194/gmd-9-1937-2016

Fosu, B. O., Wang, S.-Y. S., Wang, S.-H., Gillies, R. R., & Zhao, L. (2017). Greenhouse gases stabilizing winter atmosphere in the indo-gangetic plains may increase aerosol loading. *Atmospheric Science Letters*, *18*(4), 168–174. https://doi.org/10.1002/asl.739

Ganguly, T., Selvaraj, K. L., & Guttikunda, S. K. (2020). National clean air programme (ncap) for indian cities: Review and outlook of clean air action plans. *Atmospheric Environment: X*, *8*, 100096. https://doi.org/10.1016/j.aeaoa.2020.100096

Gani, S., Bhandari, S., Seraj, S., Wang, D. S., Patel, K., Soni, P., et al. (2019). Submicron aerosol composition in the world's most polluted megacity: The Delhi aerosol supersite study. *Atmospheric Chemistry and Physics*, *19*(10), 6843–6859. https://doi.org/10.5194/acp-19-6843-2019

Gao, C., Xiu, A., Zhang, X., Tong, Q., Zhao, H., Zhang, S., et al. (2022). Two-way coupled meteorology and air quality models in Asia: A systematic review and meta-analysis of impacts of aerosol feedbacks on meteorology and air quality. *Atmospheric Chemistry and Physics*, *22*(8), 5265–5329. https://doi.org/10.5194/acp-22-5265-2022

Gargava, P., & Rajagopalan, V. (2015a). Source apportionment studies in six indian cities—Drawing broad inferences for urban PM10 reductions. *Air Quality, Atmosphere & Health*, *9*(5), 471–481. https://doi.org/10.1007/s11869-015-0353-4

Gargava, P., & Rajagopalan, V. (2015b). Source prioritization for urban particulate emission control in India based on an inventory of PM10 and its carbonaceous fraction in six cities. *Environmental Development*, *16*, 44–53. https://doi.org/10.1016/j.envdev.2015.07.009

Government of India. (2021). Central pollution control board. Retrieved from https://app.cpcbccr.com/ccr/%23/caaqm%2Ddashboard%2Dall/caaqm%2Dlanding

Guttikunda, S. K., Goel, R., & Pant, P. (2014). Nature of air pollution, emission sources, and management in the Indian cities. *Atmospheric Environment*, *95*, 501–510. https://doi.org/10.1016/j.atmosenv.2014.07.006

Haque, M., & Singh, R. (2017). Air pollution and human health in Kolkata, India: A case study. *Climate*, *5*(4), 77. https://doi.org/10.3390/cli5040077

Hersbach, H., Bell, B., Berrisford, P., Hirahara, S., Horányi, A., Muñoz-Sabater, J., et al. (2020). The ERA5 global reanalysis. *Quarterly Journal of the Royal Meteorological Society*, *146*(730), 1999–2049. https://doi.org/10.1002/qj.3803

Hingmire, D., Vellore, R., Krishnan, R., Singh, M., Metya, A., Gokul, T., & Ayantika, D. C. (2021). Climate change response in wintertime widespread fog conditions over the indo-gangetic plains. *Climate Dynamics*, *58*(9–10), 2745–2766. https://doi.org/10.1007/s00382-021-06030-1

Horowitz, L. W., Naik, V., Paulot, F., Ginoux, P. A., Dunne, J. P., Mao, J., et al. (2020). The GFDL global atmospheric chemistry-climate model AM4.1: Model description and simulation characteristics. *Journal of Advances in Modeling Earth Systems*. https://doi.org/10.1029/2019ms002032

Horton, D. E., Skinner, C. B., Singh, D., & Diffenbaugh, N. S. (2014). Occurrence and persistence of future atmospheric stagnation events. *Nature Climate Change*, *4*(8), 698–703. https://doi.org/10.1038/nclimate2272

Hoyer, S., & Hamman, J. J. (2017). xarray: N-d labeled arrays and datasets in python. *Journal of Open Research Software*, *5*. https://doi.org/10.5334/jors.148

Hunt, K. M. R., Turner, A. G., & Shaffrey, L. C. (2018). The evolution, seasonality and impacts of Western disturbances. *Quarterly Journal of the Royal Meteorological Society*, *144*(710), 278–290. https://doi.org/10.1002/qj.3200

Hunt, K. M. R., Turner, A. G., & Shaffrey, L. C. (2019). Falling trend of Western disturbances in future climate simulations. *Journal of Climate*, *32*(16), 5037–5051. https://doi.org/10.1175/jcli-d-18-0601.1

Huszar, P., Karlický, J., Ďoubalová, J., Nováková, T., Šindelářová, K., Švábik, F., et al. (2020). The impact of urban land-surface on extreme air pollution over central Europe. *Atmospheric Chemistry and Physics*, *20*(20), 11655–11681. https://doi.org/10.5194/acp-20-11655-2020

Jethva, H., Satheesh, S. K., & Srinivasan, J. (2005). Seasonal variability of aerosols over the indo-gangetic basin. *Journal of Geophysical Research*, *110*(D21). https://doi.org/10.1029/2005jd005938

Jethva, H., Torres, O., Field, R. D., Lyapustin, A., Gautam, R., & Kayetha, V. (2019). Connecting crop productivity, residue fires, and air quality over northern India. *Scientific Reports*, *9*(1). https://doi.org/10.1038/s41598-019-52799-x

Kumar, M., Parmar, K., Kumar, D., Mhawish, A., Broday, D., Mall, R., & Banerjee, T. (2018). Long-term aerosol climatology over indo-gangetic plain: Trend, prediction and potential source fields. *Atmospheric Environment*, *180*, 37–50. https://doi.org/10.1016/j.atmosenv.2018.02.027

Kumar, M., Tiwari, S., Murari, V., Singh, A., & Banerjee, T. (2015). Wintertime characteristics of aerosols at middle Indo-Gangetic Plain: Impacts of regional meteorology and long range transport. *Atmospheric Environment*, *104*, 162–175. https://doi.org/10.1016/j.atmosenv.2015.01.014

Kumar, S., Singh, S., Shrinivasan, V., Pandey, A. K., Maddh, H. S., Shekhawat, R., et al. (2019). *Vital statistics of India based on the civil registration system (Tech. Rep.). Civil registration system section wing - A, first floor, ndcc - II building*. Jai Singh Road.

Lee, K., & Greenstone, M. (2021a). Air quality life index - India Fact Sheet (Tech. Rep.). AQLI. Retrieved from aqli.epic.uchicago.edu

Lee, K., & Greenstone, M. (2021b). Air quality life index (Tech. Rep.). AQLI. Retrieved from aqli.epic.uchicago.edu

Li, J., Hao, X., Liao, H., Hu, J., & Chen, H. (2021). Meteorological Impact on Winter $PM_{2.5}$ Pollution in Delhi: Present and Future Projection Under a Warming climate. *Geophysical Research Letters*, *48*(13). https://doi.org/10.1029/2021gl093722

Mhawish, A., Banerjee, T., Sorek-Hamer, M., Bilal, M., Lyapustin, A. I., Chatfield, R., & Broday, D. M. (2020). Estimation of high-resolution PM2.5 over the indo-gangetic plain by fusion of satellite data, meteorology, and land use variables. *Environmental Science & Technology*, *54*(13), 7891–7900. https://doi.org/10.1021/acs.est.0c01769

Midhuna, T. M., Kumar, P., & Dimri, A. P. (2020). A new Western disturbance index for the indian winter monsoon. *Journal of Earth System Science*, *129*(1). https://doi.org/10.1007/s12040-019-1324-1

Mogno, C., Palmer, P. I., Knote, C., Yao, F., & Wallington, T. J. (2021). Seasonal distribution and drivers of surface fine particulate matter and organic aerosol over the indo-gangetic plain. *Atmospheric Chemistry and Physics*, *21*(14), 10881–10909. https://doi.org/10.5194/acp-21-10881-2021

Murari, V., Kumar, M., Mhawish, A., Barman, S. C., & Banerjee, T. (2017). Airborne particulate in varanasi over middle indo-gangetic plain: Variation in particulate types and meteorological influences. *Environmental Monitoring and Assessment*, *189*(4). https://doi.org/10.1007/s10661-017-5859-9

Nair, M., Dey, S., Bherwani, H., & Ghosh, A. K. (2022). Long-term changes in aerosol loading over the 'BIHAR' state of India using nineteen years (2001–2019) of high-resolution satellite data (1x1 km2). *Atmospheric Pollution Research*, *13*(1), 101259. https://doi.org/10.1016/j.apr.2021.101259

Nair, V. S., Moorthy, K. K., Alappattu, D. P., Kunhikrishnan, P. K., George, S., Nair, P. R., et al. (2007). Wintertime aerosol characteristics over the Indo-Gangetic Plain (IGP): Impacts of local boundary layer processes and long-range transport. *Journal of Geophysical Research: Atmospheres*, *112*(D13). https://doi.org/10.1029/2006jd008099

Ojha, N., Sharma, A., Kumar, M., Girach, I., Ansari, T. U., Sharma, S. K., et al. (2020). On the widespread enhancement in fine particulate matter across the Indo-Gangetic Plain towards winter. *Scientific Reports*, *10*(1). https://doi.org/10.1038/s41598-020-62710-8

O'Neill, B. C., Kriegler, E., Riahi, K., Ebi, K. L., Hallegatte, S., Carter, T. R., et al. (2013). A new scenario framework for climate change research: The concept of shared socioeconomic pathways. *Climatic Change*, *122*(3), 387–400. https://doi.org/10.1007/s10584-013-0905-2

Pawar, H., Garg, S., Kumar, V., Sachan, H., Arya, R., Sarkar, C., et al. (2015). Quantifying the contribution of long-range transport to particulate matter (PM) mass loadings at a suburban site in the north-Western indo-gangetic plain (NW-IGP). *Atmospheric Chemistry and Physics*, *15*(16), 9501–9520. https://doi.org/10.5194/acp-15-9501-2015

Ramanathan, V., Chung, C., Kim, D., Bettge, T., Buja, L., Kiehl, J. T., et al. (2005). Atmospheric Brown clouds: Impacts on South Asian climate and hydrological cycle. *Proceedings of the National Academy of Sciences*, *102*(15), 5326–5333. https://doi.org/10.1073/pnas.0500656102

Reback, J., McKinney, W., Jbrockmendel, Van Den Bossche, J., Augspurger, T., Cloud, P., et al. (2021). pandas-dev/pandas: Pandas 1.2.4. Zenodo.

Roth, G. A., Abate, D., Abate, K. H., Abay, S. M., Abbafati, C., Abbasi, N., et al. (2018). Global, regional, and national age-sex-specific mortality for 282 causes of death in 195 countries and territories, 1980–2017: A systematic analysis for the global burden of disease study 2017. *The Lancet*, *392*(10159), 1736–1788. https://doi.org/10.1016/s0140-6736(18)32203-7

Schnell, J. L., Naik, V., Horowitz, L. W., Paulot, F., Mao, J., Ginoux, P., et al. (2018). Exploring the relationship between surface $PM_{2.5}$ and meteorology in Northern India. *Atmospheric Chemistry and Physics*, *18*(14), 10157–10175. https://doi.org/10.5194/acp-18-10157-2018

Seland, Ø., Bentsen, M., Olivié, D., Toniazzo, T., Gjermundsen, A., Graff, L. S., et al. (2020). Overview of the norwegian Earth system model (NorESM2) and key climate response of CMIP6 DECK, historical, and scenario simulations. *Geoscientific Model Development*, *13*(12), 6165–6200. https://doi.org/10.5194/gmd-13-6165-2020

Singh, N., Agarwal, S., Sharma, S., Chatani, S., & Ramanathan, V. (2021). Air pollution over India: Causal factors for the high pollution with implications for mitigation. *ACS Earth and Space Chemistry*, *5*(12), 3297–3312. https://doi.org/10.1021/acsearthspacechem.1c00170

Singh, N., Murari, V., Kumar, M., Barman, S., & Banerjee, T. (2017). Fine particulates over South Asia: Review and meta-analysis of $PM_{2.5}$ source apportionment through receptor model. *Environmental Pollution*, *223*, 121–136. https://doi.org/10.1016/j.envpol.2016.12.071

Tao, W., Liu, J., Ban-Weiss, G. A., Hauglustaine, D. A., Zhang, L., Zhang, Q., et al. (2015). Effects of urban land expansion on the regional meteorology and air quality of eastern China. *Atmospheric Chemistry and Physics*, *15*(15), 8597–8614. https://doi.org/10.5194/acp-15-8597-2015

Tatebe, H., Ogura, T., Nitta, T., Komuro, Y., Ogochi, K., Takemura, T., et al. (2019). Description and basic evaluation of simulated mean state, internal variability, and climate sensitivity in MIROC6. *Geoscientific Model Development*, *12*(7), 2727–2765. https://doi.org/10.5194/gmd-12-2727-2019

Tebaldi, C., Debeire, K., Eyring, V., Fischer, E., Fyfe, J., Friedlingstein, P., et al. (2021). Climate model projections from the scenario model intercomparison project (ScenarioMIP) of CMIP6. *Earth System Dynamics*, *12*(1), 253–293. https://doi.org/10.5194/esd-12-253-2021

Turnock, S. T., Allen, R. J., Andrews, M., Bauer, S. E., Deushi, M., Emmons, L., et al. (2020). Historical and future changes in air pollutants from CMIP6 models. *Atmospheric Chemistry and Physics*, *20*(23), 14547–14579. https://doi.org/10.5194/acp-20-14547-2020

U.S. Department of State. (2021). U.S. Embassy and Consulates' air quality monitors Retrieved from https://www.airnow.gov/international/us-embassies-and-consulates/

Verma, S., B, P., Pani, S., Kumar, D. B., Faruqi, A., Bhanja, S., & Mandal, M. (2016). Aerosol extinction properties over coastal west Bengal gangetic plain under inter-seasonal and sea breeze influenced transport processes. *Atmospheric Research*, *167*, 224–236. https://doi.org/10.1016/j.atmosres.2015.07.021

Vohra, K., Marais, E. A., Suckra, S., Kramer, L., Bloss, W. J., Sahu, R., et al. (2021). Long-term trends in air quality in major cities in the UK and India: A view from space. *Atmospheric Chemistry and Physics*, *21*(8), 6275–6296. https://doi.org/10.5194/acp-21-6275-2021

Vuuren, D. P., Kriegler, E., O'Neill, B. C., Ebi, K. L., Riahi, K., Carter, T. R., et al. (2013). A new scenario framework for climate change research: Scenario matrix architecture. *Climatic Change*, *122*(3), 373–386. https://doi.org/10.1007/s10584-013-0906-1

World Health Organization (2021). WHO global air quality guidelines. particulate matter ($PM_{2.5}$ and PM_{10}), ozone, nitrogen dioxide, sulfur dioxide and carbon monoxide.

Wu, X., Xu, Y., Kumar, R., & Barth, M. (2019). Separating Emission and meteorological Drivers of Mid-21st-century air Quality changes in India Based on Multiyear Global-Regional chemistry-climate simulations. *Journal of Geophysical Research: Atmospheres*, *124*(23), 13420–13438. https://doi.org/10.1029/2019jd030988

Yadav, S., Praveen, O. D., & Satsangi, P. G. (2015). The effect of climate and meteorological changes on particulate matter in Pune, India. *Environmental Monitoring and Assessment*, *187*(7). https://doi.org/10.1007/s10661-015-4634-z

Yang, J., Duan, K., Kang, S., Shi, P., & Ji, Z. (2016). Potential feedback between aerosols and meteorological conditions in a heavy pollution event over the Tibetan Plateau and Indo-Gangetic Plain. *Climate Dynamics*, *48*(9–10), 2901–2917. https://doi.org/10.1007/s00382-016-3240-2

Zhuang, J., Dussin, R., Huard, D., Bourgault, P., Banihirwe, A., Hamman, J., et al. (2021). pangeo-data/xesmf: v0.5.2. Zenodo. https://doi.org/10.5281/ZENODO.4464833

References From the Supporting Information

Bauer, S. E., Tsigaridis, K., Faluvegi, G., Kelley, M., Lo, K. K., Miller, R. L., & Wu, J. (2020). Historical (1850-2014) aerosol evolution and role on climate forcing using the GISS ModelE2.1 contribution to CMIP6. *Journal of Advances in Modeling Earth Systems*, *12*(8). https://doi.org/10.1029/2019ms001978

Bentsen, M., Oliviè, D. J. L., Seland, Ø., Toniazzo, T., & Gjermundsen, A. (2019b). NCC NorESM2-MM model output prepared for CMIP6 CMIP piControl. *Earth System Grid Federation*. https://doi.org/10.22033/ESGF/CMIP6.8221

Bentsen, M., Oliviè, D. J. L., Seland, Ø., Toniazzo, T., Gjermundsen, A., Graff, L. S., & Schulz, M. (2019a). NCC NorESM2-MM model output prepared for CMIP6 CMIP 1pctCO2. *Earth System Grid Federation*. 10.22033/ESGF/CMIP6.7806

Bi, D., Dix, M., Marsland, S., O'Farrell, S., Sullivan, A., Bodman, R., et al. (2020). Configuration and spin-up of ACCESS-CM2, the new generation Australian community climate and Earth system simulator coupled model. *Journal of Southern Hemisphere Earth Systems Science*, *70*(1), 225. https://doi.org/10.1071/es19040

Boucher, O., Denvil, S., Levavasseur, G., Cozic, A., Caubel, A., Foujols, M.-A., et al. (2018a). IPSL IPSL-CM6A-LR model output prepared for CMIP6 CMIP 1pctCO2. *Earth System Grid Federation*. https://doi.org/10.22033/ESGF/CMIP6.5049

Boucher, O., Denvil, S., Levavasseur, G., Cozic, A., Caubel, A., Foujols, M.-A., et al. (2018b). IPSL IPSL-CM6A-LR model output prepared for CMIP6 CMIP piControl. *Earth System Grid Federation*. https://doi.org/10.22033/ESGF/CMIP6.5251

Boucher, O., Denvil, S., Levavasseur, G., Cozic, A., Caubel, A., Foujols, M.-A., et al. (2020). IPSL IPSL-CM5A2-INCA model output prepared for CMIP6 CMIP 1pctCO2. *Earth System Grid Federation*. https://doi.org/10.22033/ESGF/CMIP6.13643

Boucher, O., Denvil, S., Levavasseur, G., Cozic, A., Caubel, A., Foujols, M.-A., et al. (2021). Ipsl ipsl-cm5a2-inca model output prepared for cmip6 cmip picontrol. *Earth System Grid Federation*. https://doi.org/10.22033/ESGF/CMIP6.13683

Boucher, O., Servonnat, J., Albright, A. L., Aumont, O., Balkanski, Y., Bastrikov, V., & Vuichard, N. (2020). Presentation and evaluation of the IPSL-CM6a-LR climate model. *Journal of Advances in Modeling Earth Systems*, *12*(7). https://doi.org/10.1029/2019ms002010

Byun, Y.-H., Lim, Y.-J., Sung, H.M., Kim, J., Sun, M., & Kim, B.-H. (2019a). NIMS-KMA KACE1.0-G model output prepared for CMIP6 CMIP 1pctCO2. *Earth System Grid Federation*. https://doi.org/10.22033/ESGF/CMIP6.8333

Byun, Y.-H., Lim, Y.-J., Sung, H.M., Kim, J., Sun, M., & Kim, B.-H. (2019b). NIMS-KMA KACE1.0-G model output prepared for CMIP6 CMIP piControl. *Earth System Grid Federation*. https://doi.org/10.22033/ESGF/CMIP6.8425

Cherchi, A., Fogli, P. G., Lovato, T., Peano, D., Iovino, D., Gualdi, S., et al. (2018). Global mean climate and main patterns of variability in the CMCC-CM2 coupled model. *Journal of Advances in Modeling Earth Systems*.

Danabasoglu, G. (2019a). NCAR CESM2 model output prepared for CMIP6 CMIP 1pctCO2. *Earth System Grid Federation*. https://doi.org/10.22033/ESGF/CMIP6.7497

Danabasoglu, G. (2019b). NCAR CESM2-WACCM model output prepared for CMIP6 CMIP 1pctCO2. *Earth System Grid Federation*. https://doi.org/10.22033/ESGF/CMIP6.10028

Danabasoglu, G. (2019c). NCAR CESM2-WACCM model output prepared for CMIP6 CMIP piControl. *Earth System Grid Federation*. https://doi.org/10.22033/ESGF/CMIP6.10094

Danabasoglu, G., Lamarque, J.-F., Bacmeister, J., Bailey, D. A., DuVivier, A. K., Edwards, J., & Strand, W. G. (2020). The community Earth system model version 2 (CESM2). *Journal of Advances in Modeling Earth Systems*, 12(2). https://doi.org/10.1029/2019ms001916

Danabasoglu, G., Lawrence, D., Lindsay, K., Lipscomb, W., & Strand, G. (2019). NCAR CESM2 model output prepared for CMIP6 CMIP piControl. *Earth System Grid Federation*. https://doi.org/10.22033/ESGF/CMIP6.7733

Dix, M., Bi, D., Dobrohotoff, P., Fiedler, R., Harman, I., Law, R., et al. (2019a). *CSIRO-ARCCSS ACCESS-CM2 model output prepared for CMIP6 CMIP 1pctCO2*. Earth System Grid Federation. https://doi.org/10.22033/ESGF/CMIP6.4230

Dix, M., Bi, D., Dobrohotoff, P., Fiedler, R., Harman, I., Law, R., et al. (2019b). *CSIRO-ARCCSS ACCESS-CM2 model output prepared for CMIP6 CMIP piControl*. Earth System Grid Federation. https://doi.org/10.22033/ESGF/CMIP6.4311

EC-Earth Consortium (EC-Earth). (2020a). EC-Earth-Consortium EC-Earth3-AerChem model output prepared for CMIP6 AerChemMIP ssp370pdSST. *Earth System Grid Federation*. Retrieved from http://cera-www.dkrz.de/WDCC/meta/CMIP6/CMIP6.AerChemMIP.EC-Earth-Consortium.EC-Earth3-AerChem.ssp370pdSST

EC-Earth Consortium (EC-Earth). (2020b). EC-Earth-Consortium EC-Earth3-AerChem model output prepared for CMIP6 AerChemMIP ssp370SST. *Earth System Grid Federation*. Retrieved from http://cera-www.dkrz.de/WDCC/meta/CMIP6/CMIP6.AerChemMIP.EC-Earth-Consortium.EC-Earth3-AerChem.ssp370SST

EC-Earth Consortium (EC-Earth). (2020c). EC-Earth-Consortium EC-Earth3-AerChem model output prepared for CMIP6 CMIP 1pctCO2. *Earth System Grid Federation*. Retrieved from http://cera-www.dkrz.de/WDCC/meta/CMIP6/CMIP6.CMIP.EC-Earth-Consortium.EC-Earth3-AerChem.1pctCO2%20doi:%2010.22033/ESGF/CMIP6.4502

EC-Earth Consortium (EC-Earth). (2020d). EC-Earth-Consortium EC-Earth3-AerChem model output prepared for CMIP6 CMIP piControl. *Earth System Grid Federation*. Retrieved from http://cera-www.dkrz.de/WDCC/meta/CMIP6/CMIP6.CMIP.EC-Earth-Consortium.EC-Earth3-AerChem.piControl%20doi:%2010.22033/ESGF/CMIP6.4843

Guo, H., John, J. G., Blanton, C., McHugh, C., Nikonov, S., Radhakrishnan, A., et al. (2018a). NOAA-GFDL GFDL-CM4 model output 1pctCO2. *Earth System Grid Federation*. https://doi.org/10.22033/ESGF/CMIP6.8470

Guo, H., John, J. G., Blanton, C., McHugh, C., Nikonov, S., Radhakrishnan, A., et al. (2018b). NOAA-GFDL GFDL-CM4 model output piControl. *Earth System Grid Federation*. https://doi.org/10.22033/ESGF/CMIP6.8666

Held, I. M., Guo, H., Adcroft, A., Dunne, J. P., Horowitz, L. W., Krasting, J., et al. (2019). Structure and performance of GFDL's CM4.0 climate model. *Journal of Advances in Modeling Earth Systems*, 11(11), 3691–3727. https://doi.org/10.1029/2019ms001829

Horowitz, L. W., Naik, V., Sentman, L., Paulot, F., Blanton, C., McHugh, C., et al. (2018a). NOAA-GFDL GFDL-ESM4 model output prepared for CMIP6 AerChemMIP ssp370pdSST. *Earth System Grid Federation*. Retrieved from http://cera-www.dkrz.de/WDCC/meta/CMIP6/CMIP6.AerChemMIP.NOAA-GFDL.GFDL-ESM4.ssp370pdSST

Horowitz, L. W., Naik, V., Sentman, L., Paulot, F., Blanton, C., McHugh, C., et al. (2018b). NOAA-GFDL GFDL-ESM4 model output prepared for CMIP6 AerChemMIP ssp370SST. *Earth System Grid Federation*. Retrieved from http://cera-www.dkrz.de/WDCC/meta/CMIP6/CMIP6.AerChemMIP.NOAA-GFDL.GFDL-ESM4.ssp370SST

Jungclaus, J., Bittner, M., Wieners, K.-H., Wachsmann, F., Schupfner, M., Legutke, S., et al. (2019a). MPI-M MPI-ESM1.2-HR model output prepared for CMIP6 CMIP 1pctCO2. Earth System Grid Federation. https://doi.org/10.22033/ESGF/CMIP6.6434

Jungclaus, J., Bittner, M., Wieners, K.-H., Wachsmann, F., Schupfner, M., Legutke, S., et al. (2019b). MPI-M MPI-ESM1.2-HR model output prepared for CMIP6 CMIP piControl. Earth System Grid Federation. https://doi.org/10.22033/ESGF/CMIP6.6674

Kelley, M., Schmidt, G. A., Nazarenko, L. S., Bauer, S. E., Ruedy, R., Russell, G. L., & Yao, M.-S. (2020). GISS-e2.1: Configurations and climatology. *Journal of Advances in Modeling Earth Systems*, 12(8). https://doi.org/10.1029/2019ms002025

Kim, Y., Noh, Y., Kim, D., Lee, M.-I., Lee, H. J., Kim, S. Y., & Kim, D. (2019a). KIOST KIOST-ESM model output prepared for CMIP6 CMIP 1pctCO2. *Earth System Grid Federation*. https://doi.org/10.22033/ESGF/CMIP6.5283

Kim, Y., Noh, Y., Kim, D., Lee, M.-I., Lee, H. J., Kim, S. Y., & Kim, D. (2019b). KIOST KIOST-ESM model output prepared for CMIP6 CMIP piControl. *Earth System Grid Federation*. https://doi.org/10.22033/ESGF/CMIP6.5303

Krasting, J. P., John, J. G., Blanton, C., McHugh, C., Nikonov, S., Radhakrishnan, A., et al. (2018a). NOAA-GFDL GFDL-ESM4 model output prepared for CMIP6 CMIP 1pctCO2. *Earth System Grid Federation*. https://doi.org/10.22033/ESGF/CMIP6.8473

Krasting, J. P., John, J. G., Blanton, C., McHugh, C., Nikonov, S., Radhakrishnan, A., et al. (2018b). NOAA-GFDL GFDL-ESM4 model output prepared for CMIP6 CMIP piControl. *Earth System Grid Federation*. https://doi.org/10.22033/ESGF/CMIP6.8669

Lee, J., Kim, J., Sun, M.-A., Kim, B.-H., Moon, H., Sung, H. M., et al. (2019). Evaluation of the Korea meteorological Administration Advanced community Earth-system model (K-ACE). *Asia-Pacific Journal of Atmospheric Sciences*, 56(3), 381–395. https://doi.org/10.1007/s13143-019-00144-7

Lovato, T., & Peano, D. (2020a). CMCC CMCC-CM2-SR5 model output prepared for CMIP6 CMIP 1pctCO2. *Earth System Grid Federation*. https://doi.org/10.22033/ESGF/CMIP6.3721

Lovato, T., & Peano, D. (2020b). CMCC CMCC-CM2-SR5 model output prepared for CMIP6 CMIP piControl. *Earth System Grid Federation*. https://doi.org/10.22033/ESGF/CMIP6.3874

Lovato, T., Peano, D., & Butenschön, M. (2021a). CMCC CMCC-ESM2 model output prepared for CMIP6 CMIP 1pctCO2. *Earth System Grid Federation*. https://doi.org/10.22033/ESGF/CMIP6.13169

Lovato, T., Peano, D., & Butenschön, M. (2021b). CMCC CMCC-ESM2 model output prepared for CMIP6 CMIP piControl. *Earth System Grid Federation*. https://doi.org/10.22033/ESGF/CMIP6.13241

Lovato, T., Peano, D., Butenschön, M., Materia, S., Iovino, D., Scoccimarro, E., & Navarra, A. (2022). mar). CMIP6 simulations with the CMCC Earth system model (CMCC-ESM2). *Journal of Advances in Modeling Earth Systems*, 14(3). https://doi.org/10.1029/2021ms002814

Mauritsen, T., Bader, J., Becker, T., Behrens, J., Bittner, M., Brokopf, R., et al. (2019). Developments in the MPI-m Earth system model version 1.2 (MPI-ESM1.2) and its response to increasing CO_2. *Journal of Advances in Modeling Earth Systems*, 11(4), 998–1038. https://doi.org/10.1029/2018ms001400

Narayanasetti, S., Gopinathan, P. A., Choudhury, A. D., Singh, M., Panickal, S., Raghavan, K., & Modi, A. (2019). CCCR-IITM IITM-ESM model output prepared for CMIP6 CMIP 1pctCO2. *Earth System Grid Federation*. Retrieved from http://cera-www.dkrz.de/WDCC/meta/CMIP6/CMIP6.CMIP.CCCR-IITM.IITM-ESM.1pctCO2%20doi:%2010.22033/ESGF/CMIP6.3515

NASA Goddard Institute For Space Studies (NASA/GISS). (2020a). NASA-GISS GISS-E2.1G model output prepared for CMIP6 AerChemMIP ssp370pdSST. *Earth System Grid Federation*. Retrieved from http://cera-www.dkrz.de/WDCC/meta/CMIP6/CMIP6.AerChemMIP.NASA-GISS.GISS-E2-1-G.ssp370pdSST

NASA Goddard Institute For Space Studies (NASA/GISS). (2020b). NASA-GISS GISS-E2.1G model output prepared for CMIP6 AerChemMIP ssp370SST. *Earth System Grid Federation*. Retrieved from http://cera-www.dkrz.de/WDCC/meta/CMIP6/CMIP6.AerChemMIP.NASA-GISS.GISS-E2-1-G.ssp370SST

Neubauer, D., Ferrachat, S., Siegenthaler-Le Drian, C., Stoll, J., Folini, D. S., Tegen, I., et al. (2019a). HAMMOZ-Consortium MPI-ESM1.2-HAM model output prepared for CMIP6 CMIP 1pctCO2. *Earth ytSystem Grid Federation*. https://doi.org/10.22033/ESGF/CMIP6.4999

Neubauer, D., Ferrachat, S., Siegenthaler-Le Drian, C., Stoll, J., Folini, D. S., Tegen, I., et al. (2019b). HAMMOZ-Consortium MPI-ESM1.2-HAM model output prepared for CMIP6 CMIP piControl. *Earth System Grid Federation*. https://doi.org/10.22033/ESGF/CMIP6.5037

Noije, T., Bergman, T., Sager, P. L., 'Donnell, D., Makkonen, R., Gonçalves-Ageitos, M., et al. (2021). EC-Earth3-AerChem: A global climate model with interactive aerosols and atmospheric chemistry participating in CMIP6. *Geoscientific Model Development*, 14(9), 5637–5668. https://doi.org/10.5194/gmd-14-5637-2021

Pak, G., Noh, Y., Lee, M.-I., Yeh, S.-W., Kim, D., Kim, S.-Y., et al. (2021). Korea institute of ocean science and technology Earth system model and its simulation characteristics. *Ocean Science Journal*, 56(1), 18–45. https://doi.org/10.1007/s12601-021-00001-7

Park, S., & Shin, J. (2019a). Snu sam0-unicon model output prepared for cmip6 cmip 1pctco2. *Earth System Grid Federation*. https://doi.org/10.22033/ESGF/CMIP6.7782

Park, S., & Shin, J. (2019b). Snu sam0-unicon model output prepared for cmip6 cmip picontrol. *Earth System Grid Federation*. Retrieved from http://cera-www.dkrz.de/WDCC/meta/CMIP6/CMIP6.CMIP.SNU.SAM0-UNICON.piControl

Park, S., Shin, J., Kim, S., Oh, E., & Kim, Y. (2019). Global climate simulated by the Seoul National University atmosphere model version 0 with a Unified Convection Scheme (SAM0-UNICON). *Journal of Climate*, 32(10), 2917–2949. https://doi.org/10.1175/jcli-d-18-0796.1

Seferian, R. (2019). CNRM-CERFACS CNRM-ESM2-1 model output prepared for CMIP6 AerChemMIP ssp370SST. *Earth System Grid Federation*. Retrieved from http://cera-www.dkrz.de/WDCC/meta/CMIP6/CMIP6.AerChemMIP.CNRM-CERFACS.CNRM-ESM2-1.ssp370SST

Seferian, R. (2020). CNRM-CERFACS CNRM-ESM2-1 model output prepared for CMIP6 AerChemMIP ssp370pdSST. *Earth System Grid Federation*. Retrieved from http://cera-www.dkrz.de/WDCC/meta/CMIP6/CMIP6.AerChemMIP.CNRM-CERFACS.CNRM-ESM2-1.ssp370pdSST

Séférian, R., Nabat, P., Michou, M., Saint-Martin, D., Voldoire, A., Colin, J., et al. (2019). Evaluation of CNRM Earth system model, CNRM-ESM2-1: Role of Earth system processes in present-day and future climate. *Journal of Advances in Modeling Earth Systems*, 11(12), 4182–4227. https://doi.org/10.1029/2019ms001791

Seland, Ø., Bentsen, M., Oliviè, D. J. L., Toniazzo, T., Gjermundsen, A., Graff, L. S., et al. (2019a). NCC NorESM2-LM model output prepared for CMIP6 CMIP 1pctCO2. *Earth System Grid Federation*. https://doi.org/10.22033/ESGF/CMIP6.7802

Seland, Ø., Bentsen, M., Oliviè, D. J. L., Toniazzo, T., Gjermundsen, A., Graff, L. S., et al. (2019b). NCC NorESM2-LM model output prepared for CMIP6 CMIP piControl. *Earth System Grid Federation*. https://doi.org/10.22033/ESGF/CMIP6.8217

Sepulchre, P., Caubel, A., Ladant, J.-B., Bopp, L., Boucher, O., Braconnot, P., et al. (2020). IPSL-CM5a2 – An Earth system model designed for multi-millennial climate simulations. *Geoscientific Model Development*, 13(7), 3011–3053. https://doi.org/10.5194/gmd-13-3011-2020

Srinivas, B., Andersson, A., Kirillova, E. N., Henry, H., Tiwari, S., Srivastava, A. K., et al. (2019). Air quality in megacity Delhi affected by countryside biomass burning. *Nature Sustainability*, 2(3), 200–205. https://doi.org/10.1038/s41893-019-0219-0

Swapna, P., Roxy, M. K., Aparna, K., Kulkarni, K., Prajeesh, A. G., Ashok, K., et al. (2015). The IITM Earth system model: Transformation of a seasonal prediction model to a long-term climate model. *Bulletin of the American Meteorological Society*, 96(8), 1351–1367. https://doi.org/10.1175/bams-d-13-00276.1

Swart, N. C., Cole, J. N., Kharin, V. V., Lazare, M., Scinocca, J. F., Gillett, N. P., et al. (2019a). CCCma CanESM5 model output prepared for CMIP6 CMIP 1pctCO2. *Earth System Grid Federation*. https://doi.org/10.22033/ESGF/CMIP6.3151

Swart, N. C., Cole, J. N., Kharin, V. V., Lazare, M., Scinocca, J. F., Gillett, N. P., et al. (2019b). CCCma CanESM5 model output prepared for CMIP6 CMIP piControl. *Earth System Grid Federation*. https://doi.org/10.22033/ESGF/CMIP6.3673

Swart, N. C., Cole, J. N. S., Kharin, V. V., Lazare, M., Scinocca, J. F., Gillett, N. P., et al. (2019c). The Canadian Earth system model version 5 (CanESM5.0.3). *Geoscientific Model Development*, 12(11), 4823–4873. https://doi.org/10.5194/gmd-12-4823-2019

Takemura, T. (2019). Miroc miroc6 model output prepared for cmip6 aerchemmip ssp370sst. *Earth System Grid Federation*. Retrieved from http://cera-www.dkrz.de/WDCC/meta/CMIP6/CMIP6.AerChemMIP.MIROC.MIROC6.ssp370SST

Takemura, T. (2020). Miroc miroc6 model output prepared for cmip6 aerchemmip ssp370pdsst. *Earth System Grid Federation*. Retrieved from http://cera-www.dkrz.de/WDCC/meta/CMIP6/CMIP6.AerChemMIP.MIROC.MIROC6.ssp370pdSST

Tatebe, H., & Watanabe, M. (2018a). MIROC MIROC6 model output prepared for CMIP6 CMIP 1pctCO2. *Earth System Grid Federation*. https://doi.org/10.22033/ESGF/CMIP6.5371

Tatebe, H., & Watanabe, M. (2018b). MIROC MIROC6 model output prepared for CMIP6 CMIP piControl. *Earth System Grid Federation*. https://doi.org/10.22033/ESGF/CMIP6.5711

Voldoire, A., Saint-Martin, D., Sénési, S., Decharme, B., Alias, A., Chevallier, M., et al. (2019). Evaluation of CMIP6 DECK experiments with CNRM-CM6-1. *Journal of Advances in Modeling Earth Systems*, 11(7), 2177–2213. https://doi.org/10.1029/2019ms001683

Volodin, E., Mortikov, E., Gritsun, A., Lykossov, V., Galin, V., Diansky, N., et al. (2019a). INM INM-CM4-8 model output prepared for CMIP6 CMIP 1pctCO2. *Earth System Grid Federation*. https://doi.org/10.22033/ESGF/CMIP6.4928

Volodin, E., Mortikov, E., Gritsun, A., Lykossov, V., Galin, V., Diansky, N., et al. (2019b). INM INM-CM4-8 model output prepared for CMIP6 CMIP piControl. *Earth System Grid Federation*. https://doi.org/10.22033/ESGF/CMIP6.5080

Volodin, E., Mortikov, E., Gritsun, A., Lykossov, V., Galin, V., Diansky, N., et al. (2019c). INM INM-CM5-0 model output prepared for CMIP6 CMIP 1pctCO2. *Earth System Grid Federation*. https://doi.org/10.22033/ESGF/CMIP6.4929

Volodin, E., Mortikov, E., Gritsun, A., Lykossov, V., Galin, V., Diansky, N., et al. (2019d). INM INM-CM5-0 model output prepared for CMIP6 CMIP piControl. *Earth System Grid Federation*. https://doi.org/10.22033/ESGF/CMIP6.5081

Volodin, E. M., Mortikov, E. V., Kostrykin, S. V., Galin, V. Y., Lykossov, V. N., Gritsun, A. S., et al. (2017). Simulation of the present-day climate with the climate model INMCM5. *Climate Dynamics*, 49(11–12), 3715–3734. https://doi.org/10.1007/s00382-017-3539-7

Volodin, E. M., Mortikov, E. V., Kostrykin, S. V., Galin, V. Y., Lykossov, V. N., Gritsun, A. S., et al. (2018). Simulation of the modern climate using the INM-CM48 climate model. *Russian Journal of Numerical Analysis and Mathematical Modelling*, 33(6), 367–374. https://doi.org/10.1515/rnam-2018-0032

Wieners, K.-H., Giorgetta, M., Jungclaus, J., Reick, C., Esch, M., Bittner, M., et al. (2019a). MPI-M MPI-ESM1.2-LR model output prepared for CMIP6 CMIP 1pctCO2. Earth System Grid Federation. https://doi.org/10.22033/ESGF/CMIP6.6435

Wieners, K.-H., Giorgetta, M., Jungclaus, J., Reick, C., Esch, M., Bittner, M., et al. (2019b). MPI-M MPI-ESM1.2-LR model output prepared for CMIP6 CMIP piControl. Earth System Grid Federation. https://doi.org/10.22033/ESGF/CMIP6.6675

Yukimoto, S., Kawai, H., Koshiro, T., Oshima, N., Yoshida, K., Urakawa, S., et al. (2019). The meteorological Research Institute Earth system model version 2.0, MRI-ESM2.0: Description and Basic Evaluation of the Physical Component. *Journal of the Meteorological Society of Japan. Ser. II*, *97*(5), 931–965. https://doi.org/10.2151/jmsj.2019-051

Yukimoto, S., Koshiro, T., Kawai, H., Oshima, N., Yoshida, K., Urakawa, S., et al. (2019a). MRI MRI-ESM2.0 model output prepared for CMIP6 AerChemMIP ssp370SST. *Earth System Grid Federation*. Retrieved from http://cera-www.dkrz.de/WDCC/meta/CMIP/CMIP6.AerChem-MIP.MRI.MRI-ESM2-0.ssp370SST

Yukimoto, S., Koshiro, T., Kawai, H., Oshima, N., Yoshida, K., Urakawa, S., et al. (2019b). MRI MRI-ESM2.0 model output prepared for CMIP6 CMIP 1pctCO2. *Earth System Grid Federation*. https://doi.org/10.22033/ESGF/CMIP6.5356

Yukimoto, S., Koshiro, T., Kawai, H., Oshima, N., Yoshida, K., Urakawa, S., et al. (2019c). MRI MRI-ESM2.0 model output prepared for CMIP6 CMIP piControl. *Earth System Grid Federation*. https://doi.org/10.22033/ESGF/CMIP6.6900

Yukimoto, S., Koshiro, T., Kawai, H., Oshima, N., Yoshida, K., Urakawa, S., et al. (2020). MRI MRI-ESM2.0 model output prepared for CMIP6 AerChemMIP ssp370pdSST. *Earth System Grid Federation*. Retrieved from http://cera-www.dkrz.de/WDCC/meta/CMIP/CMIP6.AerChem-MIP.MRI.MRI-ESM2-0.ssp370pdSST

Zhao, M., Golaz, J.-C., Held, I. M., Guo, H., Balaji, V., Benson, R., et al. (2018). The GFDL global atmosphere and land model AM4.0/LM4.0 - 1. simulation characteristics with prescribed SSTs. *Journal of Advances in Modeling Earth Systems*. https://doi.org/10.1002/2017ms001208

Ziehn, T., Chamberlain, M., Lenton, A., Law, R., Bodman, R., Dix, M., et al. (2019a). CSIRO ACCESS-ESM1.5 model output prepared for CMIP6 CMIP 1pctCO2. Earth System Grid Federation. https://doi.org/10.22033/ESGF/CMIP6.4231

Ziehn, T., Chamberlain, M., Lenton, A., Law, R., Bodman, R., Dix, M., et al. (2019b). CSIRO ACCESS-ESM1.5 model output prepared for CMIP6 CMIP piControl. Earth System Grid Federation. https://doi.org/10.22033/ESGF/CMIP6.4312

Ziehn, T., Chamberlain, M. A., Law, R. M., Lenton, A., Bodman, R. W., Dix, M., et al. (2020). The Australian Earth system model: ACCESS-ESM1.5. *Journal of Southern Hemisphere Earth Systems Scienc*e, *70*(1), 193. https://doi.org/10.1071/es19035